© NOV 2025 | IRE Journals | Volume 9 Issue 5 | ISSN: 2456-8880
DOI: https://doi.org/10.64388/IREV9I5-1712275

# Structural And Thermal Properties of Quaternary $B_2O_3$ – $Na_2O$ – RO–$MnO_2$ (R=Mg, Zn, Cd) GLASSES

R. AMARAVEL[1], L. BALU[2], R. EZHIL PAVAI[3], T KAVITHA[4], R BHUVANESHWARI[5]
*Department of Physics, St Joseph's college (Arts & Science) Kovur Chennai.*
*Department of Physics, Govaerts college, Chidambram.Tamilnadu.*
*Department of Physics, Thiru Kolanjiappar Government Arts College, Virudhachalam, Tamilnadu*

***Abstract-*** ***The quaternary glass systems of $B_2O_3$ – $Na_2O$ – RO – $MnO_2$ (R=Mg, Zn, Cd) with different compositions of $MnO_2$ are prepared by melt-quenching technique. Amorphous nature of these glasses has been confirmed from their XRD profiles. Density of all the glass samples is measured using relative measurement method. FTIR spectra of these glasses are recorded over a continuous spectral range (4000 – 400 cm-1) as an attempt to study their structural units. Thermal properties of the glasses are studied using differential thermal analysis. The longitudinal and shear ultrasonic velocities are measured for all the compositions at 303K and at 10MHz frequency using the Pulse Echo Overlap method. Elastic moduli and other parameters such as molar volume, Poisson's ratio, acoustic impedance, microhardness and Debye temperature are calculated from density and velocity data, and they are used to gain knowledge about the structural and mechanical properties of these glasses, and are correlated with the rigidity and compactness of the glass systems***

***Keywords: XRD, FTIR, -DTA and Ultrasonic Studies***

## I. INTRODUCTIONS

Transition metal ions (TMIs) containing glasses have attracted great attention because of their numerous applications in memory switching, electrical threshold and optical switching devices (1-3). TMIs are considered as effective and useful dopant ions in the glass materials owing to the fact that they exist in different valance states with different co-ordinations simultaneously in the glass network, which is mainly responsible for bringing significant changes in the physical properties and structural modifications in the glass system (4). Among transition metal oxides, manganese oxide has strong bearing on optical, electrical and magnetic properties (5), and has been widely studied due to their technological importance for catalytic and electrochemical applications (6). Manganese ion is used to probe glass structure, since it exhibits different valance states from +2 to +7 ($Mn^{2+}$ ($3d^5$), $Mn^{3+}$ ($3d^4$), $Mn^{4+}$ ($3d^3$) and $Mn^{5+}$ ($3d^2$)) in different glass matrices depending on quantitative properties of glass formers and modifiers, ion size in glass matrix, field strength and mobility of the modifier cation.

Generally, the optical, electrical/semiconducting and magnetic properties arise from electron/polaron hoping between different valence states of ions from lower to the higher state. $Mn^{3+}$ and $Mn^{2+}$ are well known paramagnetic ions while $Mn^{2+}$ and $Mn^{4+}$ are luminescent activators. Trivalent manganese ($Mn^{3+}$) ion in glasses exhibits octahedral coordination having large magnetic anisotropy due to its strong spin-orbit interaction of the 3d orbit, whereas divalent manganese ($Mn^{2+}$) ion with tetrahedral and octahedral coordination possesses small magnetic anisotropy due to zero angular momentum (7).

Borate glasses containing manganese ions have been under extensive investigation because of their technological applications especially in microelectronics, optical glasses and solid state laser (7-10). Many workers have investigated the structural role of $MnO_2$ in glasses (10-12) prepared the PbO – ZnO – $B_2O_3$ - $MnO_2$ glasses and studied their properties. They observed that when the concentration of $MnO_2$ in the glass network is low upto 0.4 mol%, manganese ions seem to exist mainly in $Mn^{2+}$ state and occupy network forming positions and strengthen the glass structure. If the concentration is increased gradually, these ions seen to exist mainly in $Mn^{3+}$ state and occupy modifying positions thereby increasing disorder in the glass network.In the present study, an effort is made to understand the changes that occur in the structure and elastic properties with the addition of manganese oxide into a ternary BNR glass systems at the expense of divalent oxide content through ultrasonic measurements.

© NOV 2025 | IRE Journals | Volume 9 Issue 5 | ISSN: 2456-8880
DOI: https://doi.org/10.64388/IREV9I5-1712275

## II. EXPERIMENTAL DETAILS

Glass samples belong to BNRMn ($70B_2O_3$ – (30-x)$Na_2O$ – (x-y)RO – y$MnO_2$), where x=5,15,20 and 25 mol% and y=1,2,3,4 and 5 mol% respectively, R=MgO, ZnO, CdO] are prepared using the technique described in Chapter II in the temperature range 800-950°C using $B_2O_3$, $Na_2O$, MgO, ZnO, CdO and $MnO_2$ as starting materials of reagent purity grade. Glass samples belonging to some borate based binary and ternary glass systems. namely Quaternary glass were prepared by melt quench technique using the starting materials as $B_2O_3$, $Na_2O$, MgO, ZnO, CdO and $MnO_2$, of reagent purity grade. The required amount (approximately 20g) in mol% of different chemicals in powder form was weighed using a single pan balance having an accuracy of ± 0.001g. The homogenization of the appropriate mixture of the components of chemicals is effected by repeated grinding using a mortar. The homogeneous mixture is put in a silica crucible and placed in a furnace. Melting is carried out under controlled conditions at a temperature from 750 to 1010ºC for all the systems. The molten mixture was cast into a copper mould having the dimension of 10mm diameter and 6mm thickness. Then the glass samples were annealed at 450ºC for two hours to avoid the mechanical strain developed during the quenching process. The prepared glass samples were polished and the surfaces were made perfectly plane and smoothened by diamond disc and diamond powder. The samples prepared were chemically stable and non-hygroscopic.

The nomenclature and composition of BNRMn glass samples are given in Table 1.0 and the photographs of the prepared glasses are displayed in Plates 1.1 - 1.2

Table 1.0. Nomenclature and composition of quaternary glass systems

| Plate | Nomenclature | Composition in mol % | Remarks |
|---|---|---|---|
| 1.0 | $B_2O_3$ – $Na_2O$ – MgO – $MnO_2$ | | Mol% of $B_2O_3$ is constant |
| | BNMMn1 | 70-25-04-1 | |
| | BNMMn2 | 70-20-08-2 | |
| | BNMMn3 | 70-15-12-3 | |
| | BNMMn4 | 70-10-16-4 | |
| | BNMMn5 | 70-05-20-5 | |
| 1.1 | $B_2O_3$ – $Na_2O$ – ZnO – $MnO_2$ | | |
| | BNZMn1 | 70-25-04-1 | |
| | BNZMn2 | 70-20-08-2 | |
| | BNZMn3 | 70-15-12-3 | |
| | BNZMn4 | 70-10-16-4 | |
| | BNZMn5 | 70-05-20-5 | |
| 1.2 | $B_2O_3$ – $Na_2O$ – CdO – $MnO_2$ | | |
| | BNCMn 1 | 70-25-04-1 | |
| | BNCMn 2 | 70-20-08-2 | |
| | BNCMn 3 | 70-15-12-3 | |
| | BNCMn 4 | 70-10-16-4 | |
| | BNCMn 5 | 70-05-20-5 | |

© NOV 2025 | IRE Journals | Volume 9 Issue 5 | ISSN: 2456-8880
DOI: https://doi.org/10.64388/IREV9I5-1712275

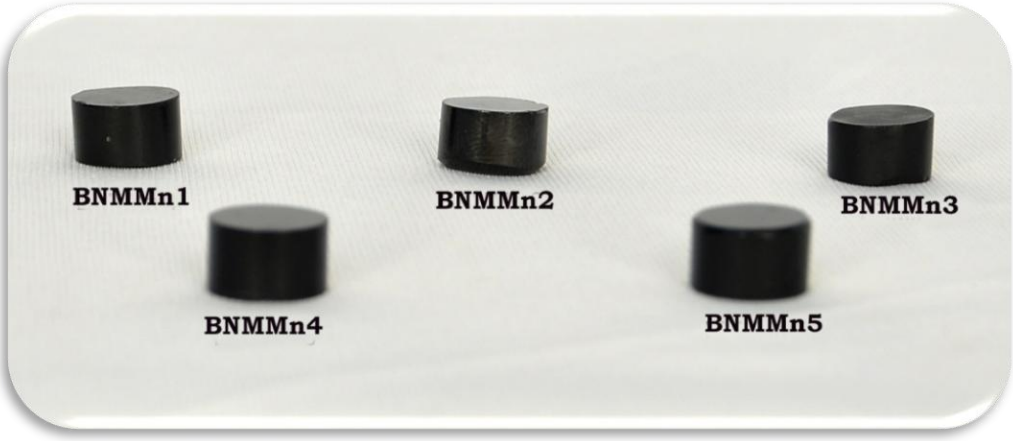


Plate 1.0. Photograph of BNMMn glass samples

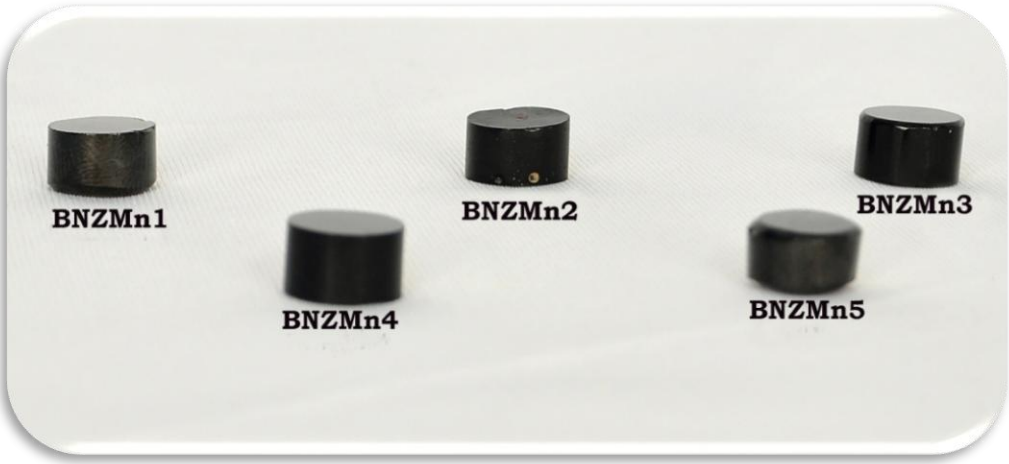


Plate 1.1. Photograph of BNZMn glass samples

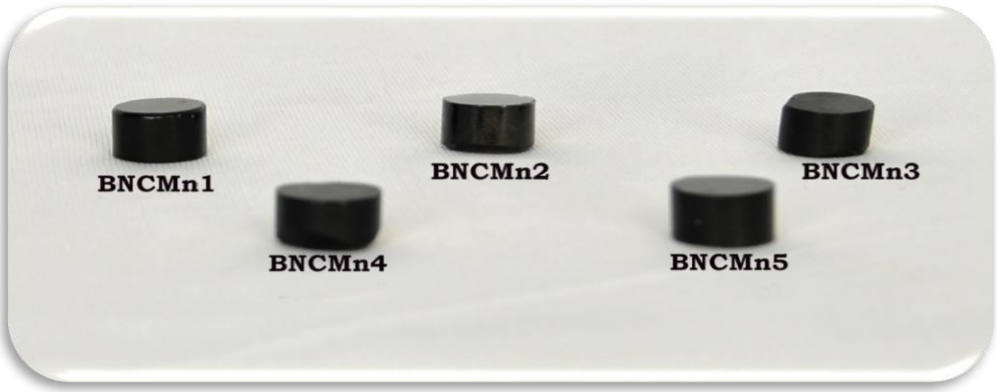


Plate 1.2. Photograph of BNCMn glass samples

## III. RESULTS AND DISCUSSION

XRD pattern of BNMMn, BNZMn and BNCMn glasses

The XRD pattern of BNMMn, BNZMn and BNCMn glasses is shown in Fig.1.0. The X-ray spectrograms show no continuous or discrete sharp peak, but exhibit broad halo, which reflects the characteristics of amorphous glass structures. The absence of long-range atomic arrangement is a clear indication of the amorphous nature of the glass samples (13).

© NOV 2025 | IRE Journals | Volume 9 Issue 5 | ISSN: 2456-8880
DOI: https://doi.org/10.64388/IREV9I5-1712275

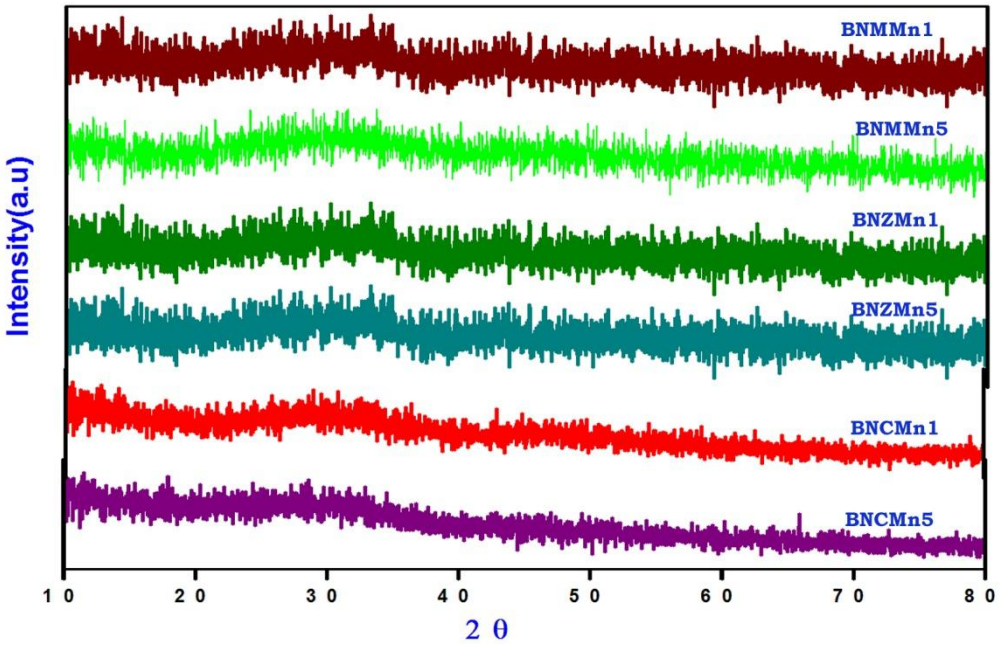


Fig. 1.0 XRD pattern of BNMMn, BNZMn and BNCMn glasses

FTIR Analysis

Fourier transform infrared spectroscopy is used to analyse the local structural changes occurring in the vitreous network such as breaking or rearrangement of chemical bonds with the addition of manganese to ternary sodium borate glass network. Important changes in the properties of glass can occur as a result of structural transformation. Figs.1.1,1.2 and 1.3 depict the FTIR spectra of BNRMn (R=Mg, Zn, Cd) glass systems and the assignments of the detected absorption band as summarized in Table. 1.1.

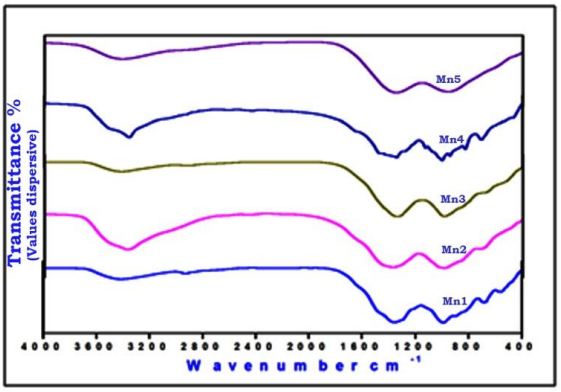


Fig1.11 FTIR spectra for BNMMn glasses with different concentration $MnO_2$

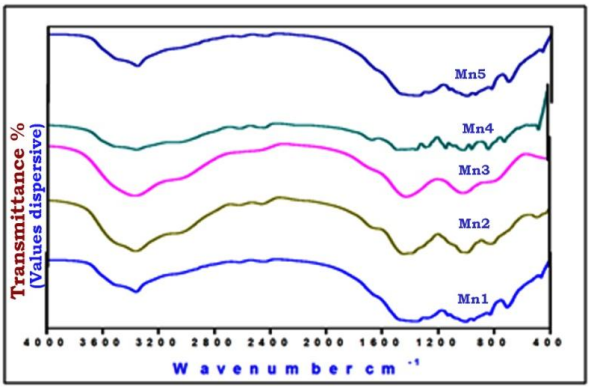


Fig1.2 FTIR spectra for BNZMn glasses with different concentration $MnO_2$

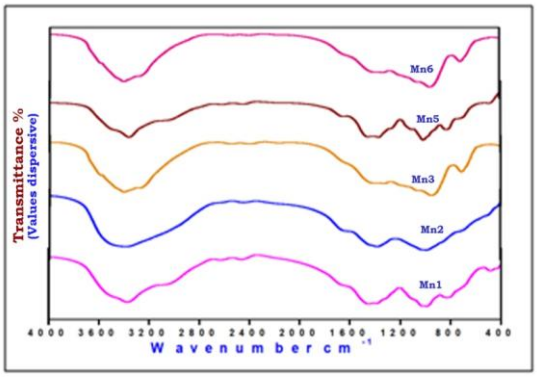


Fig. 1.3 FTIR spectra for BNCMn glasses with different concentration

© NOV 2025 | IRE Journals | Volume 9 Issue 5 | ISSN: 2456-8880
DOI: https://doi.org/10.64388/IREV9I5-1712275

Table 1.1 Band positions and their corresponding assignments of infrared spectra of BNMMn, BNZMn and BNCMn glass systems

| Wavenumber $cm^{-1}$ | Assignment | References |
|---|---|---|
| ~ 1352-1383 | B-O stretching vibrations of the trigonal $BO_3$ unit | |
| ~ 991-1160 | B-O stretching vibrations of the tetrahedral $BO_4$ | Lakshminarayana and Buddhudu, 2006 |
| ~608-714 | Bending vibrations of B-O-B linkages | Ezhil Pavai and Kiruthika Devi, 2016 |
| ~462-497 | Vibration of metal cation $Mn^{2+}$ | Manisha Pal, et al., 2011 |

In the present glasses, the bands from 1352 to 1383$cm^{-1}$ are characteristic of the stretching vibrations of B-O in $BO_3$ triangles. The vibrational band located in the region 991-1160 $cm^{-1}$ is due to stretching vibrations of tetrahedral $BO_4$ units. The additional shoulder peak centered at ~608-714$cm^{-1}$ is assigned to B-O-B bending vibration of $BO_3$ groups.

The absorption band appeared around 400-600 $cm^{-1}$ in the glass samples due to the specific vibrations of divalent metal cations in all glasses network. In general, the bands around 3200-3800 $cm^{-1}$ in the present glass systems are assigned to OH stretching vibration and this group is usually present in all borate glasses.

In the BNRMn (R=Mg, Zn) glasses, the stretching vibration of trigonal $BO_3$ units is shifted to higher intensities upto 3 mol% of manganese and it implies that manganese ion is located near B-O vibration (ie weak B-O-Mn linkage is possible). At higher concentration of manganese (x>3mol%), the intensity of $BO_3$ units decreases and this is ascribed to decrease in the length of R-O bonds due to vicinity of manganese, thus, the energy of vibration increases. The opposite behavior is observed in the stretching vibration of tetraderal $BO_4$ units. The intensity of this band decreases initially, and then increases with the continuous incorporation of $MnO_2$ in the BRMNn/BRZMn glass matrix.

In the present BNCMn glass matrix, the band between 1063-1102 $cm^{-1}$ represents vibrations of B-O bonds is $BO_3$ units. This band exhibits a shift to lower wave number. The bands at 1350-1378 $cm^{-1}$ are due to the stretching vibration of $BO_4$ units and the intensities of this peak increase with increase of $MnO_2$ concentration (14) indicating an increase in the formation $BO_4$ unit with bridging oxygen (B-O-Mn). The shifts and the intensity change in the properties of this glass system.

6.3 THERMAL ANALYSIS

DTA provides information on glass transition temperature ($T_g$) which indicates structural changes associated with change in composition ($MnO_2$ content), because it is very sensitive to change in coordination number of network forming atoms and non-bridging oxygens. Generally the effect of cations on $T_g$ is related to (i) the density of covalent cross-linking, (ii) oxygen density of the network, (iii) the number and strength of the cross-links between oxygen and cation.

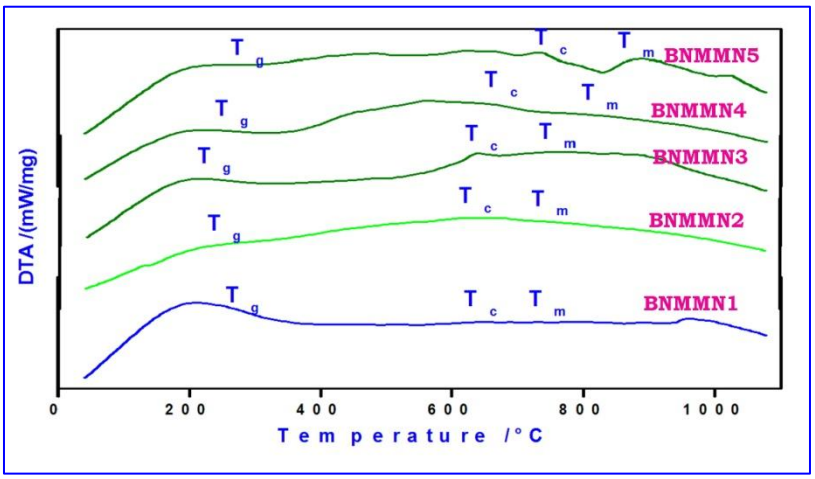


Fig. 1.4 DTA curves of BNMMn glasses

© NOV 2025 | IRE Journals | Volume 9 Issue 5 | ISSN: 2456-8880
DOI: https://doi.org/10.64388/IREV9I5-1712275

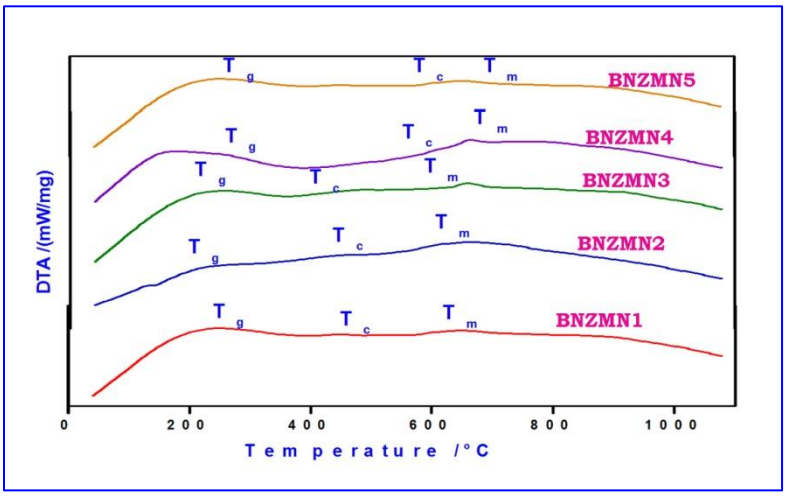


Fig. 1.5 DTA curves of BNZMn glasses

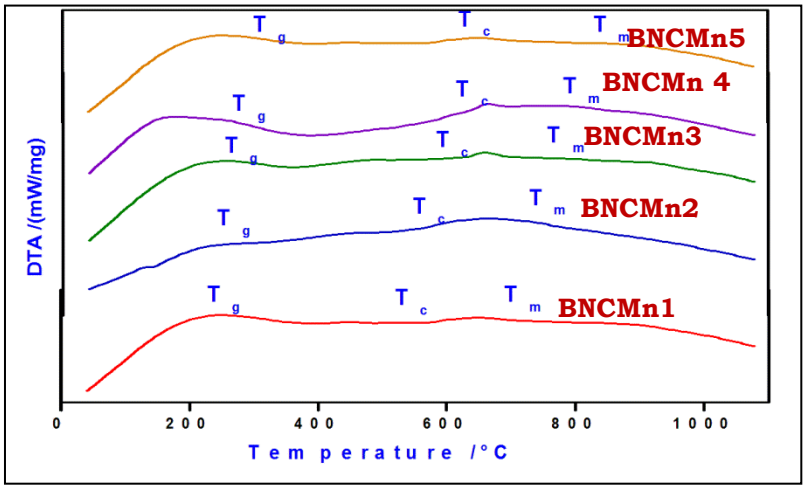


Fig. 1.6 DTA curves of BNCMn glasses

Table.1.3 Values of glass transition temperature($T_g$), crystallization temperature($T_c$), melting temperature($T_m$), thermal stability (s) and Hruby's parameter ($Kg_{l)}$ of BNRMn glass system

| Name of the sample | Glass transition temperature (°C) | Crystallization temperature (°C) | Melting temeprature (°C) | Thermal stability | Hruby's parameter |
|---|---|---|---|---|---|
| $B_2O_3$ – $Na_2O$ – MgO | | | | | |
| BNMMn1 | 275 | 669 | 770 | 394 | 3.90 |
| BNMMn2 | 270 | 659 | 760 | 389 | 3.85 |
| BNMMn3 | 259 | 646 | 758 | 387 | 3.46 |
| BNMMn4 | 275 | 667 | 790 | 392 | 3.19 |
| BNMMn5 | 308 | 720 | 830 | 412 | 3.75 |
| $B_2O_3$ – $Na_2O$ – ZnO | | | | | |
| BNZMn1 | 260 | 471 | 645 | 211 | 1.25 |
| BNZMn2 | 247 | 451 | 640 | 204 | 1.14 |
| BNZMn3 | 237 | 435 | 630 | 198 | 1.07 |
| BNZMn4 | 284 | 572 | 620 | 288 | 2.23 |

| | | | | | |
|---|---|---|---|---|---|
| BNZMn5 | 292 | 601 | 701 | 309 | 2.47 |
| $B_2O_3 – Na_2O – CdO$ | | | | | |
| BNCMn1 | 255 | 550 | 724 | 295 | 1.70 |
| BNCMn2 | 275 | 574 | 747 | 299 | 1.73 |
| BNCMn3 | 290 | 604 | 782 | 314 | 1.76 |
| BNCMn4 | 310 | 628 | 798 | 318 | 1.87 |
| BNCMn5 | 316 | 671 | 851 | 335 | 1.97 |

From DTA profiles as shown in Figs.1.4,1.5 1.6 the transition temperature, crystallization temperature and melting temperature decrease upto 3 mol% of $MnO_2$ and then for higher concentration $x \geq 3$ mol %, it increases exhibiting maximum for 5 mol% of $MnO_2$. This trend is explained as follows, the initial decrease in $T_g$ $T_c$ and $T_m$ for $MnO_2$ concentration upto 5 mol% is because manganese ion occupies network modifying position and distrupts the closely packed borate structure (breaks the oxygen bonding) and results in increase of non-bridging oxygens. As a result the structure expands and the rigidity of the glass decreases. Increase in characteristic temperature beyond 3 mol% of $MnO_2$ is due to the formation of high degree of cross-links with tetrahedral coordinated borate ($BO_4$) units, decreasing volume and enhancing rigidity of the glass structure. Above 3 mol% manganese ion occupies network forming position. The S and $Kg_1$ values show similar trend.

The DTA curves for BMCMn glasses in Fig. 1.5 show a small endothermic hump corresponding to the glass transition temperature at 260°C, and this is followed by an exothermic peak corresponding to crystallization temperature at 471°C and other endothermic events corresponding to the melting temperature at 645°C. The values of $T_g$, $T_c$ and $T_m$ increase with increasing manganese ion at the expense of cadmium ion. The substitution of manganese ions in place of cadmium ions strengthens the borate network and hence the glass structure.

From the application point of view, the glass should be thermally stable. This thermal stability of the glass can be estimated on the basis of calorimetric measurements using DTA. Generally, unstable glasses show crystallization peak close to the glass transition temperature. Therefore, the temperature difference ($T_c$-$T_g$) is a good indication of thermal stability because the higher the value of this difference causes delayed in nucleation (15). From the measured values of $T_g$, $T_c$ and $T_m$, the glass stability factor (s) and Hruby's parameters (Kgl) are calculated and shown in Table 1.3. The gradual replacement of CdO by $MnO_2$ increase the values of S and $Kg_l$. The maximum value of stability and Hruby's parameter for BNCMn5 glasses indicates their highest thermal stability and glass forming ability among the glasses under investigation.

BNRMn (R=Mg, Zn) glass systems

The density, molar volume, longitudinal velocity and shear velocity of the different glass specimens with respect to change in mol% of $MnO_2$ are listed in Table 1.4. The calculated longitudinal modulus (L), shear modulus (G), bulk modulus (K), Young's modulus (E) and Poisson's ratio (σ) are reported in Table 1.5 The acoustic impedance (Z), microhardness (H) and Debye temperature ($\theta_D$) are presented in Table 1.5

Figs. 1.6 to 2.1 show the variation of density, molar volume, longitudinal velocity and shear velocity with different composition of $MnO_2$ for the BNMMn and BNZMn glass systems. The variation of elastic moduli and the remaining parameters for both the systems are depicted in Figs. 1.5 and 1.6 show the variation of measured and evaluated parameter of BNCMn glass system.

The useful information regarding short range structure of glasses can be obtained by density and molar volume measurements. It can be seen from the Table 1.6 that the density and molar volume show a non-linear variation with increase in $MnO_2$ content but oppositely directed. The density values initially decrease upto 3 mol% of $MnO_2$ and then increase with the increase of $MnO_2$ concentration. The change in density of such systems is related to the formed structural units when introducing the modifier oxide.

© NOV 2025 | IRE Journals | Volume 9 Issue 5 | ISSN: 2456-8880
DOI: https://doi.org/10.64388/IREV9I5-1712275

Table 1.4 Values of density, molar volume, longitudinal velocity and shear velocity of BNMMn and BNZMn glass systems

| Name of the sample | Density $\rho$ ($10^3$kgm$^{-3}$) | Molar Volume $V_m$( $10^{-6}$m$^3$/mol) | Ultrasonic velocity (ms$^{-1}$) | |
|---|---|---|---|---|
| | | | Longitudinal ($U_l$) | Shear ($U_s$) |
| $B_2O_3 + Na_2O + MgO + MnO_2$ | | | | |
| BNMMn1 | 2.759 | 26.5 | 5591.3 | 3070.9 |
| BNMMn2 | 2.699 | 30.0 | 5440.2 | 2957.2 |
| BNMMn3 | 2.483 | 32.7 | 5210.8 | 2801.8 |
| BNMMn4 | 2.541 | 26.4 | 5453.4 | 2985.3 |
| BNMMn5 | 2.802 | 24.1 | 5684.6 | 3130.8 |
| $B_2O_3 + Na_2O + ZnO + MnO_2$ | | | | |
| BNZMn1 | 2.629 | 23.4 | 5250.1 | 2851.3 |
| BNZMn2 | 2.439 | 25.3 | 5065.0 | 2745.7 |
| BNZMn3 | 2.391 | 29.2 | 4920.5 | 2632.3 |
| BNZMn4 | 2.656 | 25.2 | 5132.9 | 2782.3 |
| BNZMn5 | 2.703 | 24.6 | 5346.8 | 3033.5 |

The non-linear variation in density is reflected in molar volume as shown in Figs 2.25-2.40 which is attributed to the rearrangement of structure with the addition of $MnO_2$ into the glasses. This explains the strengthening of glass network.

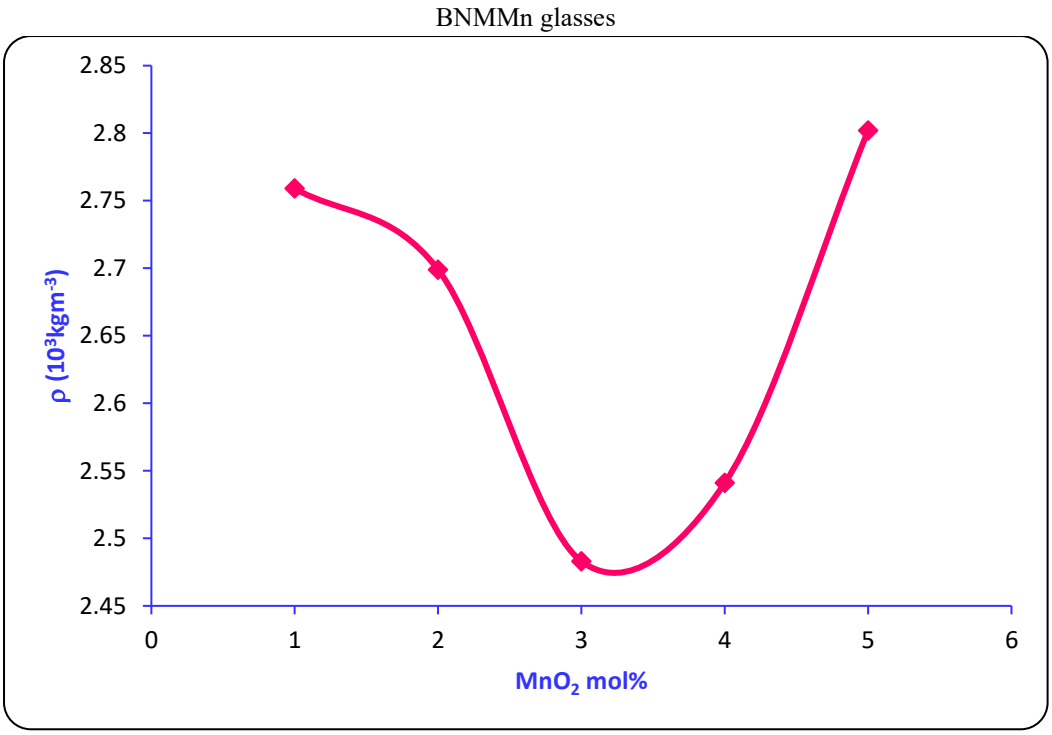


Fig. 1.6 Variation of density with $MnO_2$ mol%

© NOV 2025 | IRE Journals | Volume 9 Issue 5 | ISSN: 2456-8880
DOI: https://doi.org/10.64388/IREV9I5-1712275

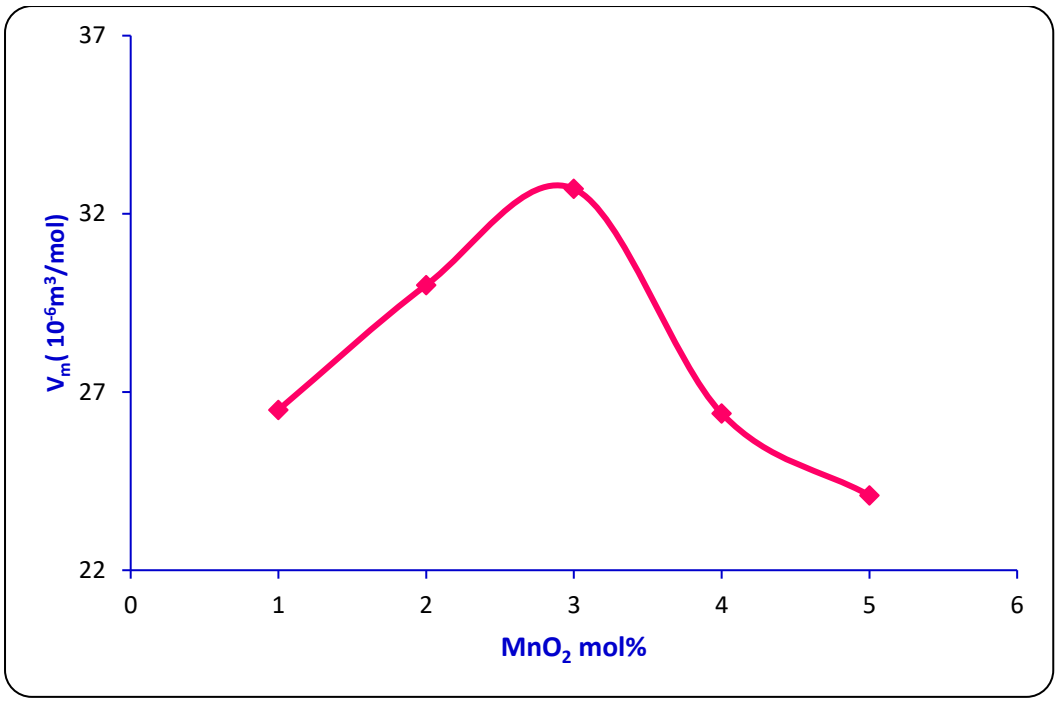


Fig. 1.7 Variation of molar volume with $MnO_2$ mol%

Figs.2.4 show the values of ultrasonic velocities of BNMMn and BNZMn glass systems as a function of $MnO_2$ concentration. The addition of $MnO_2$ into BNR structure shows that the longitudinal and shear velocities decrease upto 3 mol%. This indicates that the managnese ions resides in the BNR glass matrix as glass modifier results in the structural rearrangement of glasses due to the formation of NBO and this leads to decrease in the connectivity of the glass network. Then, the progressive addition of $MnO_2$ content shows an increase in both velocities. The observed increase in ultrasonic velocities can be explained such that, as manganese ions enter interstitially, some type of modification occurs in the already existing B-O-Na and B – O – R linkages into new covalent B–O–Mn linkages. The addition of $MnO_2$ content contributes to a volume contraction which is reflected in density and molar volume results.

BNZMn glasses

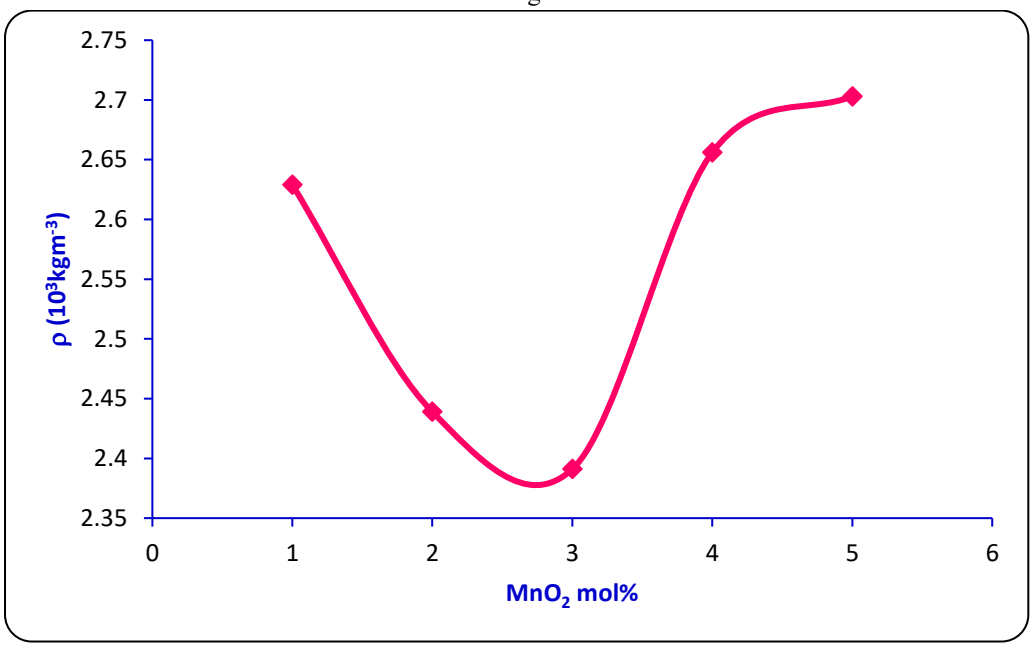


Fig. 1.8 Variation of density with $MnO_2$ mol%

© NOV 2025 | IRE Journals | Volume 9 Issue 5 | ISSN: 2456-8880
DOI: https://doi.org/10.64388/IREV9I5-1712275

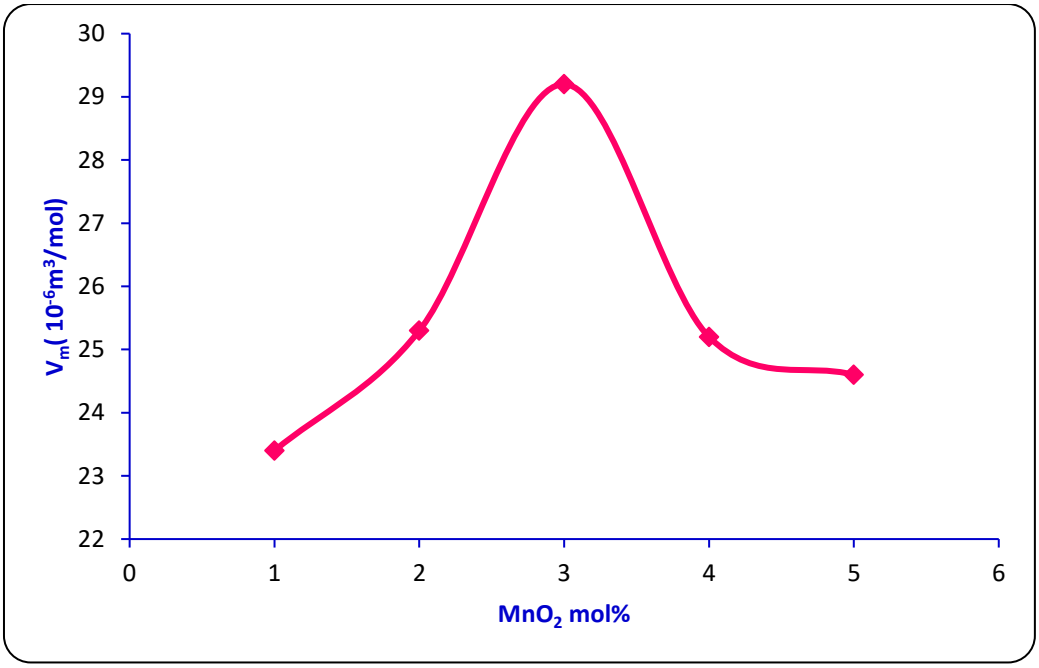


Fig. 1.9. Variation of molar volume with $MnO_2$ mol%

BNMMn glasses

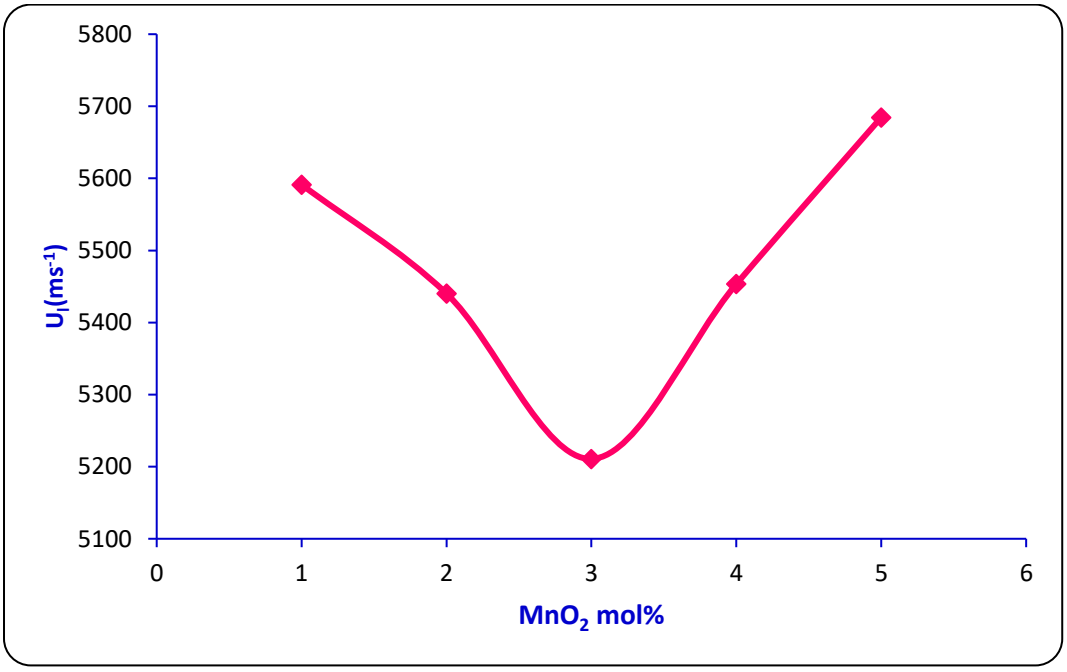


Fig. 2.0 Variation of longitudinal velocity with $MnO_2$ mol%

© NOV 2025 | IRE Journals | Volume 9 Issue 5 | ISSN: 2456-8880
DOI: https://doi.org/10.64388/IREV9I5-1712275

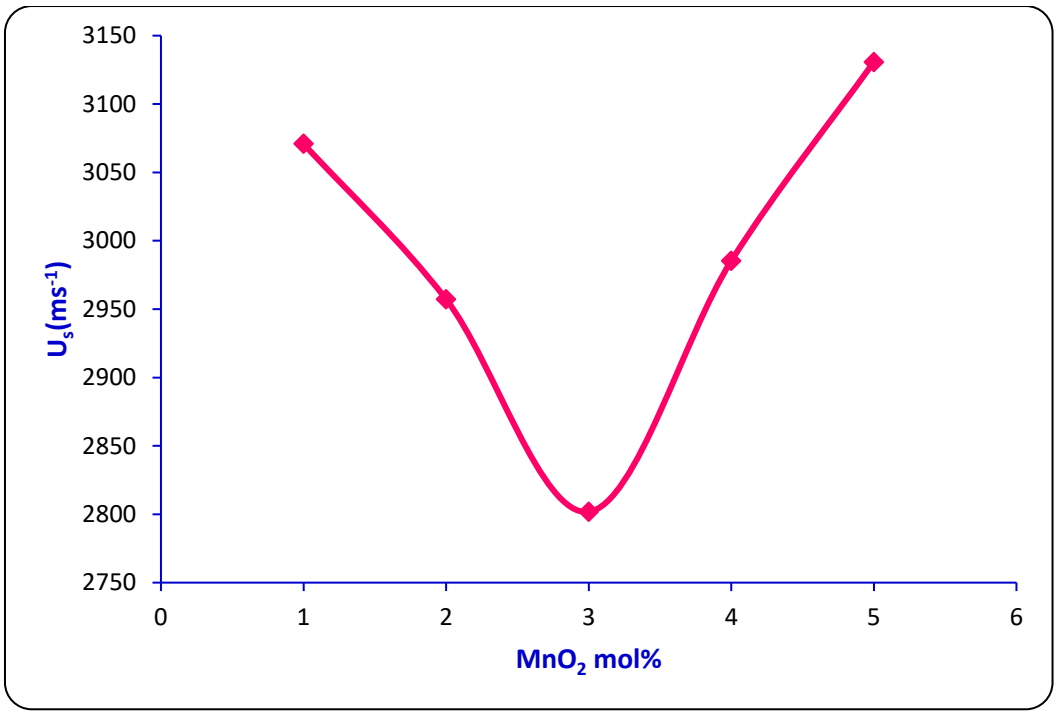


Fig. 2.1 Variation of shear velocity with $MnO_2$ mol%

BNZMn glasses

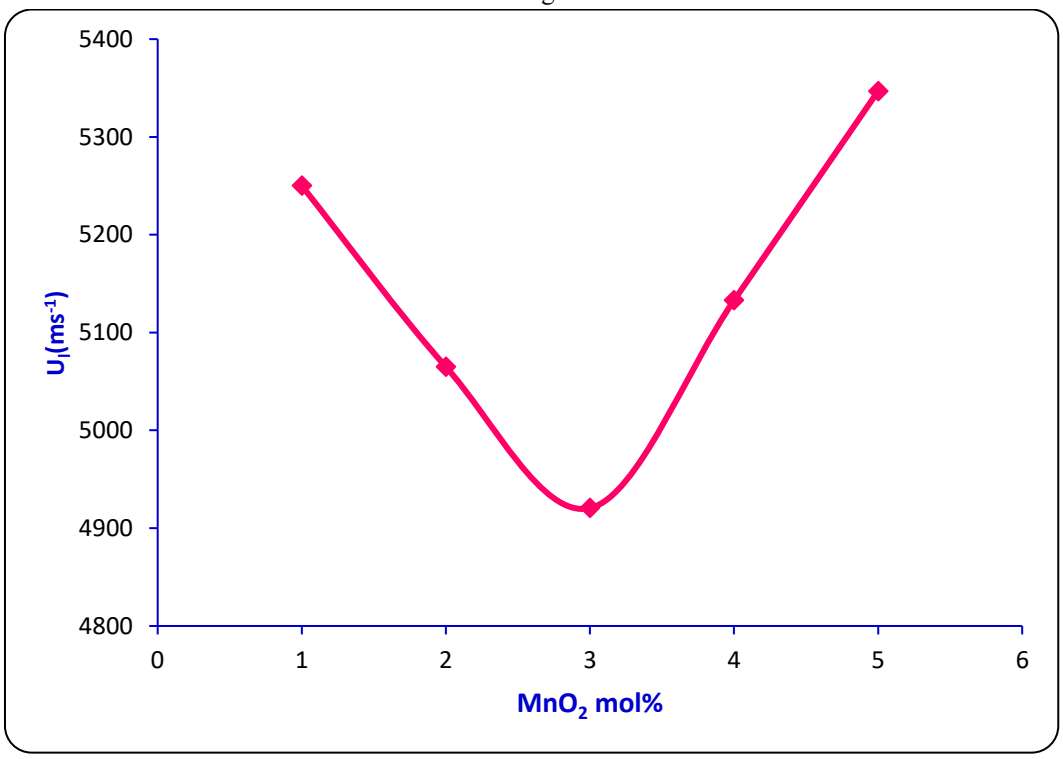


Fig. 2.22Variation of longitudinal velocity with $MnO_2$ mol%

© NOV 2025 | IRE Journals | Volume 9 Issue 5 | ISSN: 2456-8880
DOI: https://doi.org/10.64388/IREV9I5-1712275

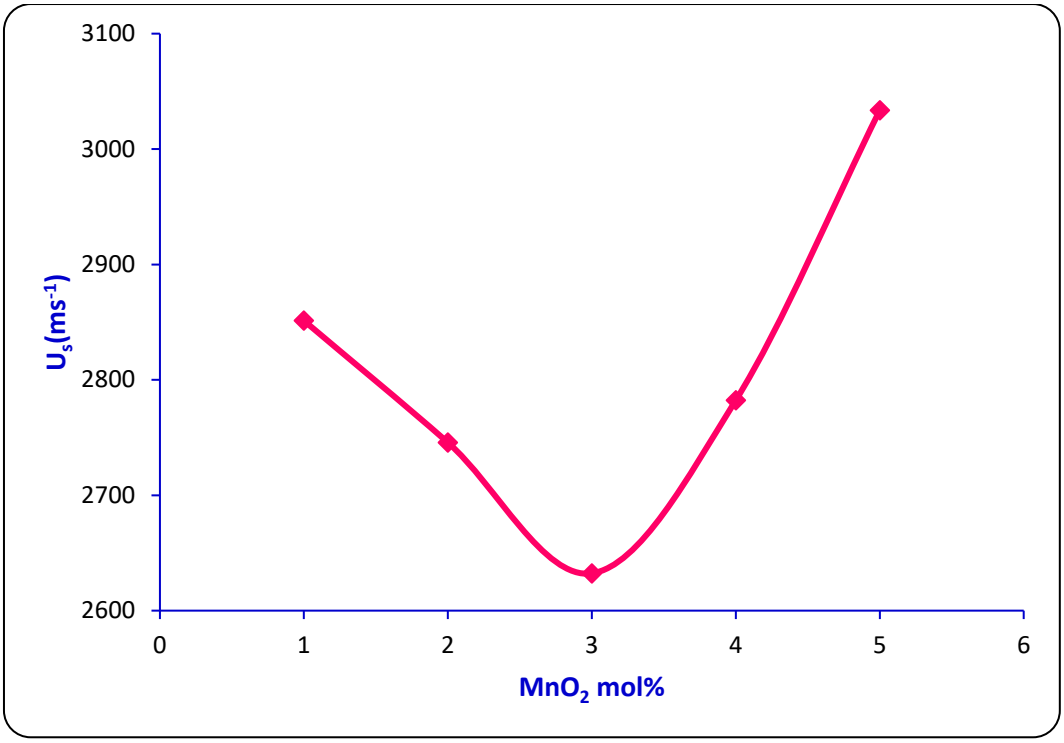


Fig. 2.23 Variation of shear velocity with $MnO_2$ mol%

BNMMn glasses

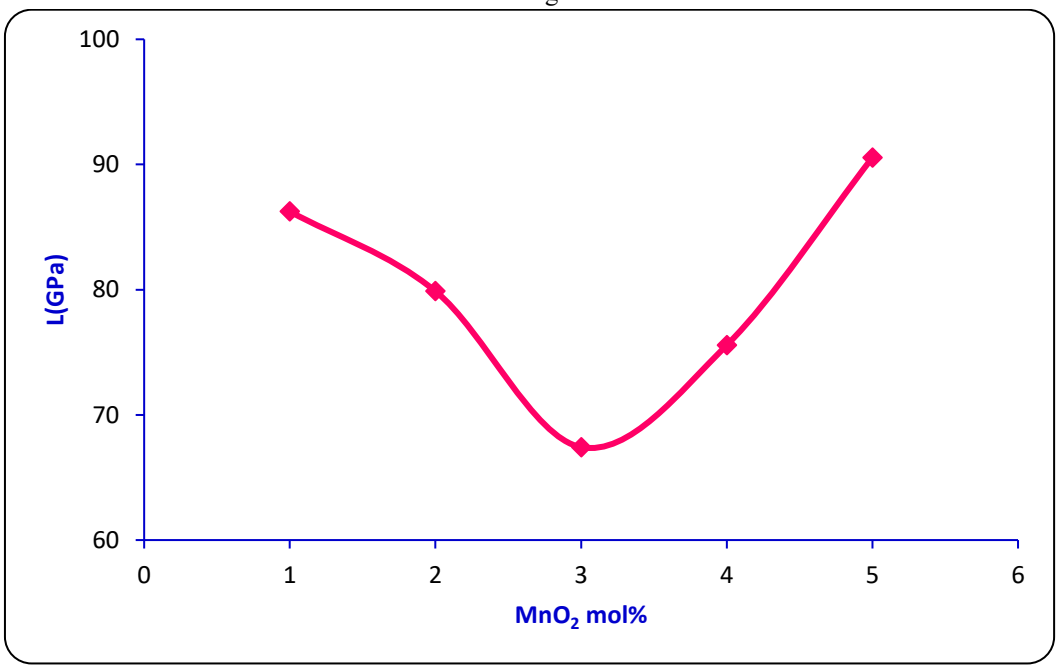


Fig. 2.24 Variation of longitudinal modulus with $MnO_2$ mol%

© NOV 2025 | IRE Journals | Volume 9 Issue 5 | ISSN: 2456-8880
DOI: https://doi.org/10.64388/IREV9I5-1712275

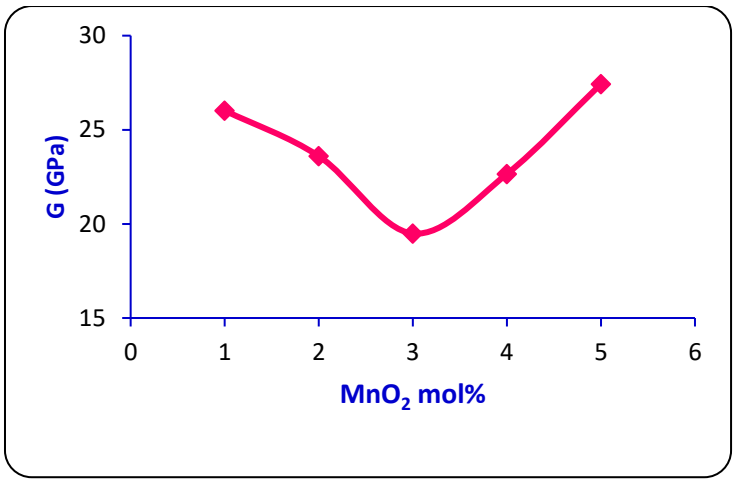


Fig2.25 Variation of shear modulus with $MnO_2$ mol%

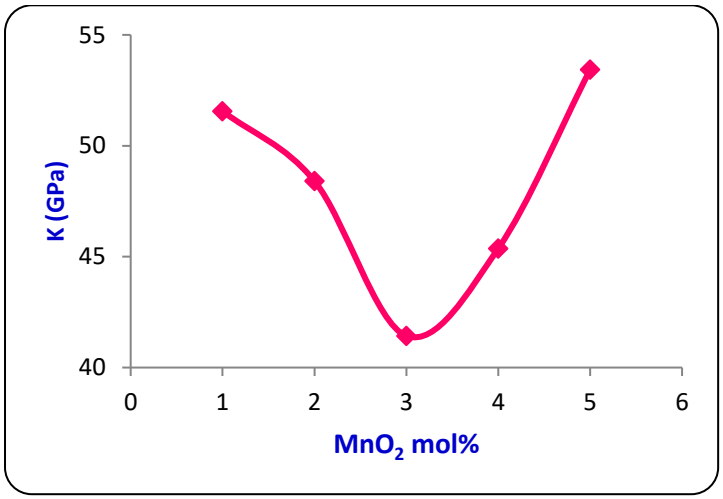


Fig. 2.26 Variation of bulk modulus with $MnO_2$ mol%

BNZMn glasses

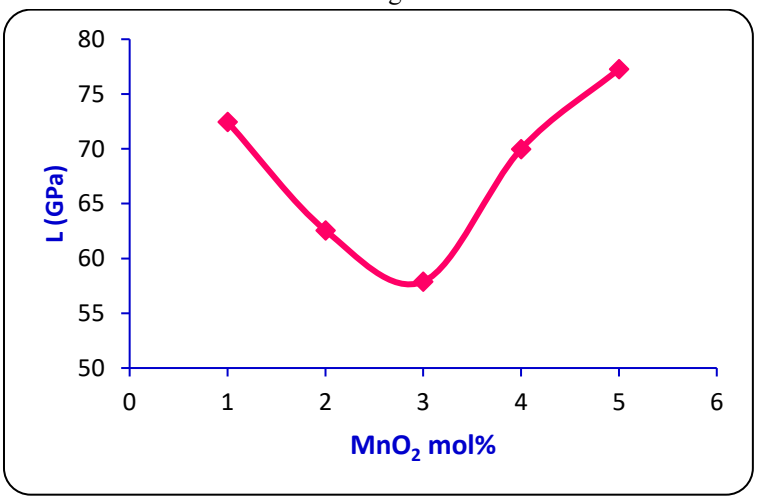


Fig. 2.27 Variation of longitudinal modulus with $MnO_2$ mol%

© NOV 2025 | IRE Journals | Volume 9 Issue 5 | ISSN: 2456-8880
DOI: https://doi.org/10.64388/IREV9I5-1712275

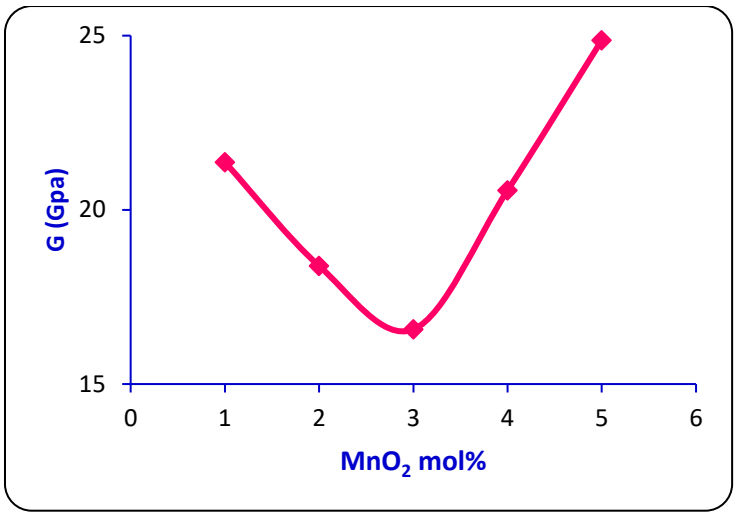


Fig2.28 Variation of shear modulus with $MnO_2$ mol%

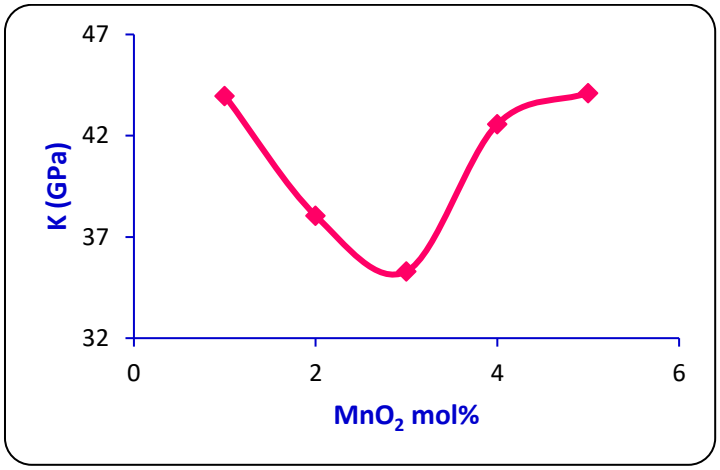


Fig. 2.30 Variation of bulk modulus with $MnO_2$ mol%

BNMMn glasses

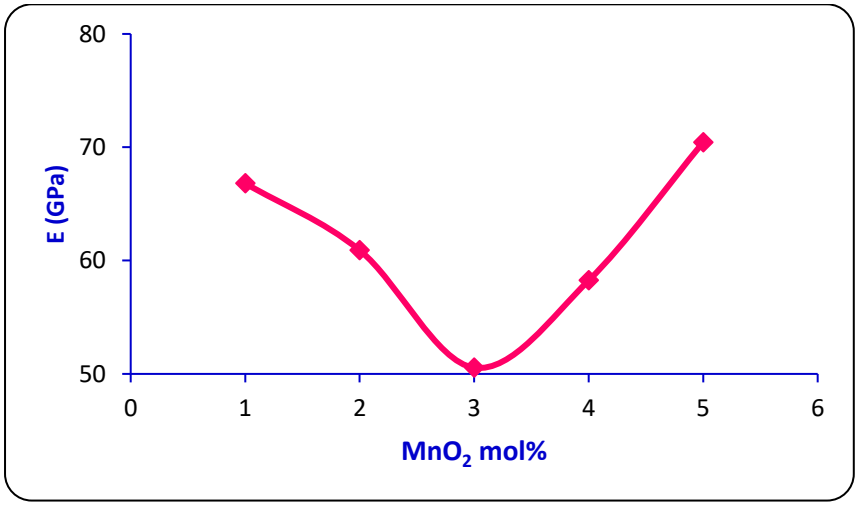


Fig. 2.31 Variation of Young's modulus with $MnO_2$ mol%

© NOV 2025 | IRE Journals | Volume 9 Issue 5 | ISSN: 2456-8880
DOI: https://doi.org/10.64388/IREV9I5-1712275

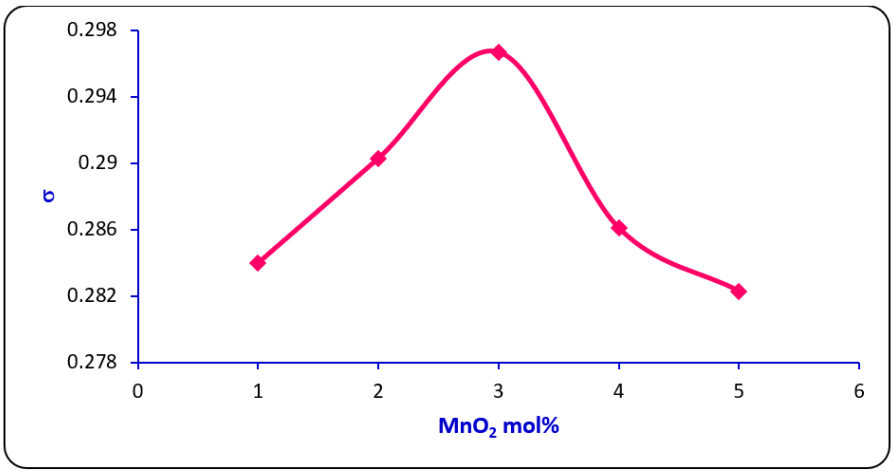


Fig. 2.32 Variation of Poisson's ratio with $MnO_2$ mol%

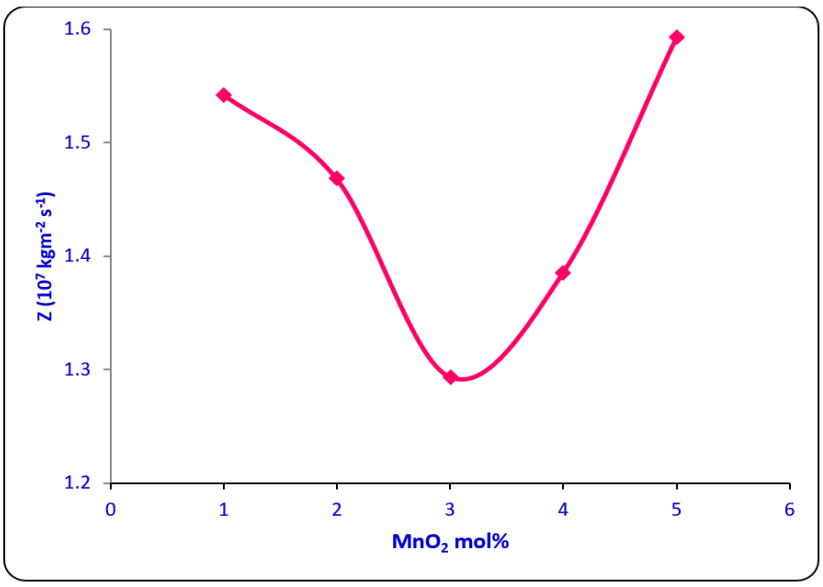


Fig. 2.33 Variation of acoustic impedance with $MnO_2$ mol%

BNZMn glasses

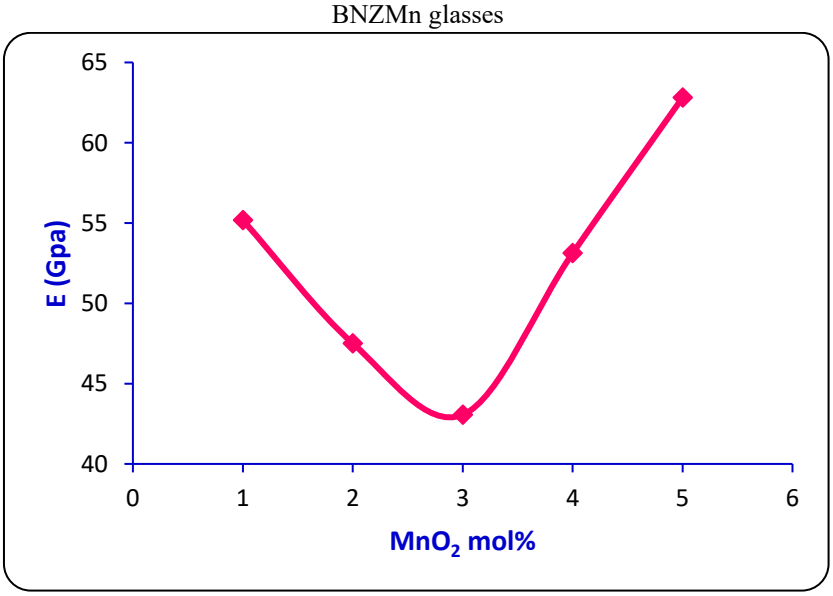


Fig. 2.34 Variation of Young's modulus with $MnO_2$ mol%

© NOV 2025 | IRE Journals | Volume 9 Issue 5 | ISSN: 2456-8880
DOI: https://doi.org/10.64388/IREV9I5-1712275

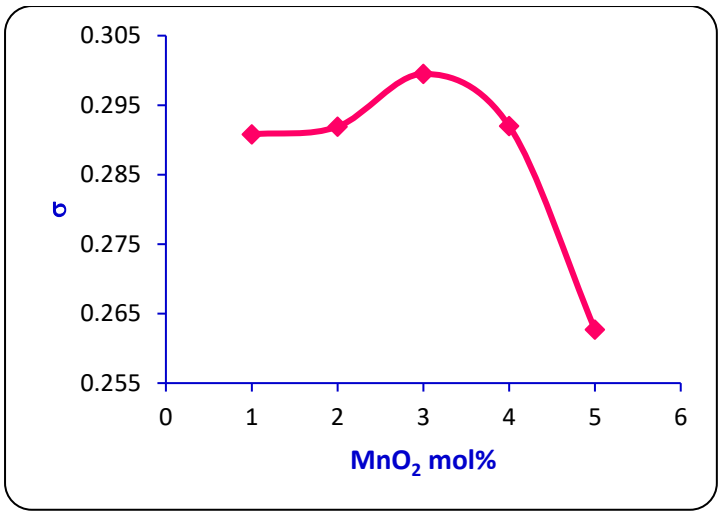


Fig. 2.35 Variation of Poisson's ratio with $MnO_2$ mol%

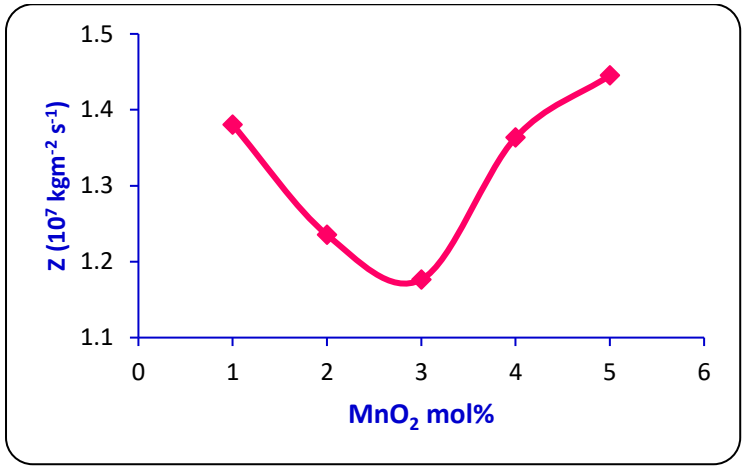


Fig. 2.36 Variation of acoustic impedance with $MnO_2$ mol%

BNMMn glasses

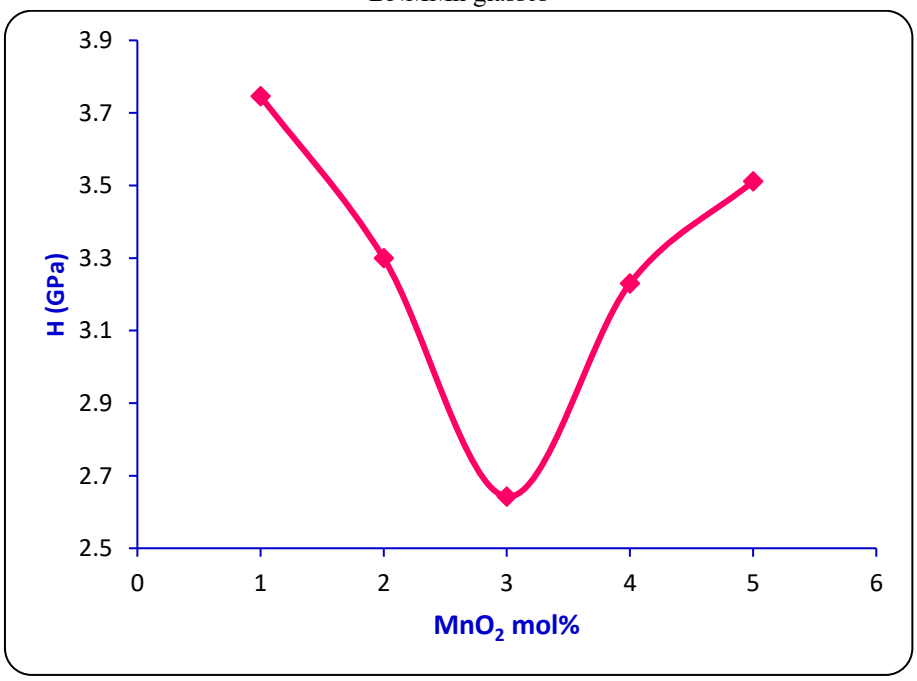


Fig. 2.37 Variation of microhardness with $MnO_2$ mol%

© NOV 2025 | IRE Journals | Volume 9 Issue 5 | ISSN: 2456-8880
DOI: https://doi.org/10.64388/IREV9I5-1712275

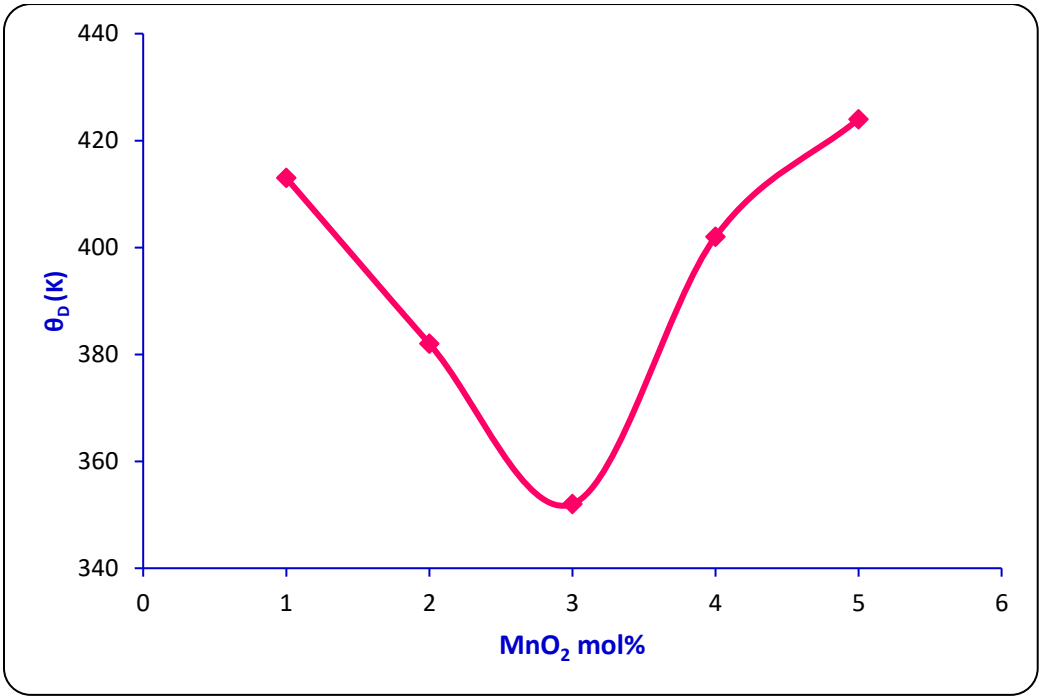


Fig. 2.38 Variation of Debye temperature with $MnO_2$ mol%

BNZMn glasses

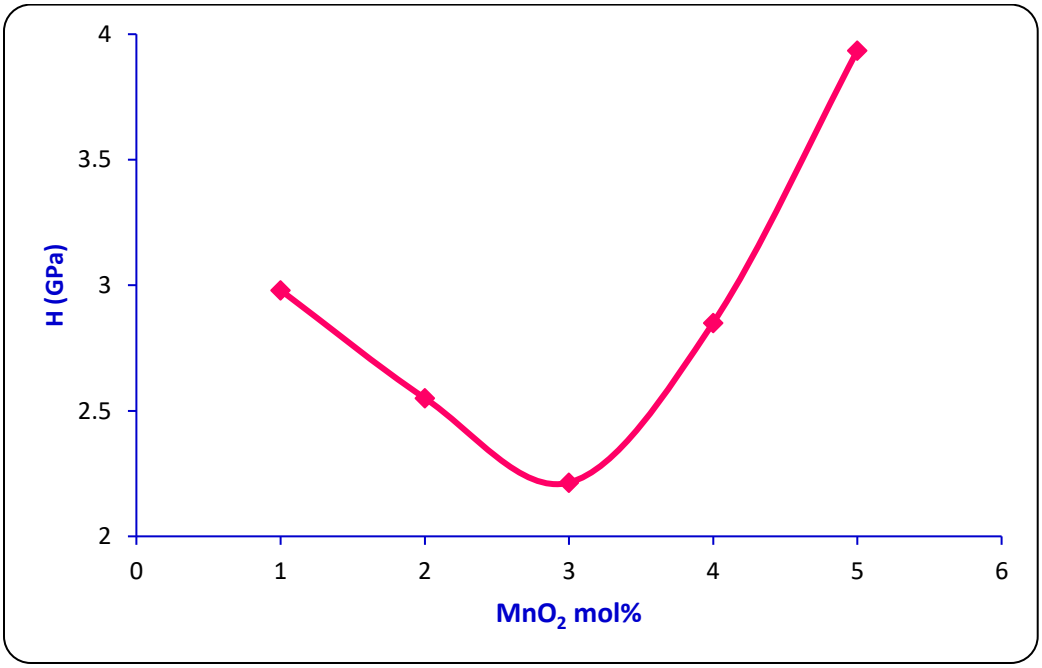


Fig. 2.39 Variation of microhardness with $MnO_2$ mol%

© NOV 2025 | IRE Journals | Volume 9 Issue 5 | ISSN: 2456-8880
DOI: https://doi.org/10.64388/IREV9I5-1712275

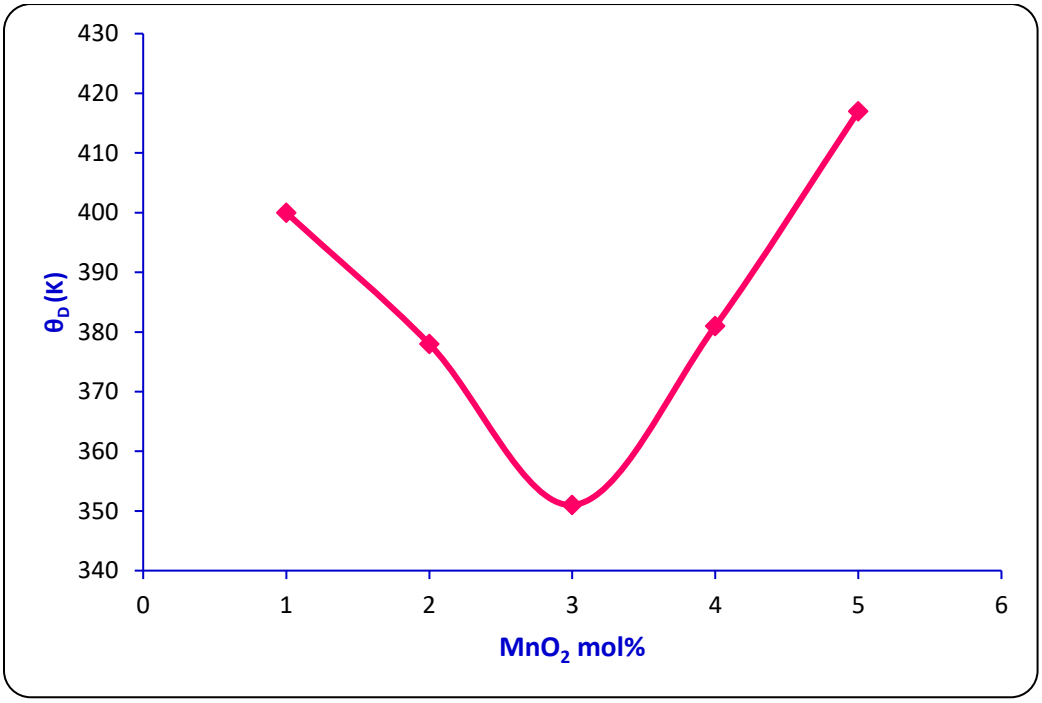


Fig. 2.40 Variation of Debye temperature with $MnO_2$ mol%

Figs.2.10-2.40 show the variation of elastic moduli of studied glass systems as a function of $MnO_2$ concentration. It is observed that the ultrasonic velocities decrease upto 3mol% of $MnO_2$ and subsequently increase when incorporation of $MnO_2$ is greater than 3mol% in divalent oxide doped sodium borate network. The elastic moduli variations are similar to the variation of the ultrasonic velocity with composition.

It is evident from the figures that the elastic moduli decrease at lower concentration of $MnO_2$. With further addition of $MnO_2$, the manganes ions start to take part in the formation of glass matrix. This indicates that the manganese oxide acts as network modifier up to 3 mol% and x > 3mol% and it acts as network former.

The Poisson's ratio is a measure of cross-link density of the glass system. The change in cross-link density of the glass network is well understandable from the variations in Poisson's ratio. Figs. 2.31-2.40 show the variation of Poisson's ratio (σ) with $MnO_2$ concentration. It can be seen from the figures that the Poisson's ratio increases from BNRMn1 glass to BNRMn3 glass, which indicates decrease in cross-linking of the network (i.e., formation of ionic Mn-O bonds). The Poisson's ratio decreases for BNRMn4 and BNRMn5 glasses, it represents the strength of glasses is increased (16).

The non-linear variation of acoustic impedance (Z) with increase in $MnO_2$ content is as shown in Table 1.5. the acoustic impedance is found to be low 3 mol% of $MnO_2$. The gradual decrease in the value is due to the increasing formation of non-bridging oxygen atoms, resulting in decrease in the strength of the glass network. Above 3mol% of $MnO_2$ content, it increases.

Figs. 2.39-2.40 show the dependence of microhardness (H) with $MnO_2$ concentration in the BNRMn glasses. With the addition of $MnO_2$, glasses showed decrease in microhardness at 3 mol% it reflects the weakening of glass network, upto this concentration. Further addition of $MnO_2$ (X>3 mol%) in the glass result in reverse trend and this indicates the stronger bonding developed in the glass network. On the other hand, the large increase in H at higher concentration of $MnO_2$ is related to the increase of bridging oxygens in the glass matrix, which strengths the network and leads to increase in the stress to eliminate free volume.

Table 1.6 shows that the Debye temperature decreases with increase in concentration ($x \geq 3$ mol %) of $MnO_2$. This is mainly due to the increase in the number of non-bridging oxygens as a direct effect of the insertion of manganese ions into the glass network. This supports well over earlier conclusion derived from the previous parameters.

The progressive replacement of divalent ions by manganese ions has caused a decrease in the values of measured and evaluated parameters (except Poisson's ratio, which is inversely proportional to elastic moduli) upto 3mol%. In this position, the manganese ions behave as a network modifier with $MnO_6$ octahedral structure. Beyond 3 mol% it takes part into the glass network as a former in the form of $MnO_4$ tetrahdral structure, connected to neighbouring $BO_4$ by bridging oxygen (B-O-Mn bonds). Both magnesium and zinc ions have same size, coordination number and charge. BNRMn glasses with MgO content show highest values of ultrasonic parameters compared to ZnO content. This is due to the highest covalent character of magnesium ions in the glass network.

## IV. CONCLUSION

The physical and elastic properties of BNRMn (R = MgO, ZnO) glass systems have been investigated to explore the role of $MnO_2$ in the glass network.

- The density, ultrasonic velocities, elastic moduli and other parameters decrease with the addition of $MnO_2$ content upto 3 mol%. This shows a decrease in the connectivity of the glass network while on further addition of $MnO_2$, all these parameters and hence connectivity of the network increase.
- Poisson's ratio indicates that $MnO_2$ is effective in the formation of cross-linking between cations for above 3 mol%, which contributes to the increase in stiffness and rigidity of the glass.
- $MnO_2$ plays a role of glass modifier at lower composition, while it exhibits glass former at high concentration in the studied glasses.
- BNRMn glasses with MgO content have high covalent character in the glass network and produce more compact glass structure.
- IR spectra confirm the presence of borate and manganese structural units.
- It is found from thermal properties that manganese ions are incorporated in the glass network as network modified and network former. This behavior depends on the variation of composition and nature of the components.